Novel acryloylated and methacryloylated nanocellulose derivatives with improved mucoadhesive properties

Macromolecular Bioscience
www.mbs-journal.de

Novel Acryloylated and Methacryloylated Nanocellulose Derivatives with Improved Mucoadhesive Properties

Abdumutolib A. Atakhanov, Nurbek Sh. Ashurov, Makhliyo M. Kuzieva, Burhon N. Mamadiyorov, Doniyor J. Ergashev, Sayyora Sh. Rashidova, and Vitaliy V. Khutoryanskiy**

In this work, three nanocellulose derivatives are synthesized with the aim of preparing new mucoadhesive materials. Nanocellulose is reacted with glycidyl methacrylate in dimethylsulphoxide, and with acryloyl and methacryloyl chloride in dimethylacetamide in the presence of 4-(N,N-dimethylamino)pyridine as a catalyst. These reactions are carried out under heterogeneous conditions, and the reaction products are characterized using various spectroscopic techniques, X-ray diffraction, atomic force microscopy, and thermogravimetric analysis. The Fourier-transform infrared spectra showed all the characteristic absorption bands typical for cellulose and also new peaks at 1720 cm^{-1} for the carbonyl group (C═O) and 1639, 812 cm^{-1} for the double bond (C═C). It is established that the crystal structure of the nanocellulose is slightly changed with derivatisation and the thermal stability of these derivatives increased. Mucoadhesive properties of nanocellulose and its derivatives is evaluated using the tensile test, rotating basket method, and fluorescence flow-through method. The retention of these polymers is evaluated on sheep oral mucosal tissue ex vivo using artificial saliva. Test results demonstrated that the new derivatives of nanocellulose have improved mucoadhesive properties compared to the parent nanocellulose.

1. Introduction

Cellulose is the most abundant natural and renewable biopolymer on earth. It has attracted more and more attention in different fields and could serve as a useful alternative for the exhaustible fossil resources, owing to its biodegradability and environmental friendliness.[1–3] Modified form of cellulose—nanocellulose (NC) exhibits good mechanical properties, low density, nanoscale dimensions, high surface area, biocompatibility, and low toxicity and has a great potential to be used in many areas, such as electronics,[4] biosensor technology,[5] polymer composites,[6–9] pharmacy,[10] and biomedicine.[11–13] NC can be extracted from different cellulose sources (wood, cotton, kenaf, bamboo, sisal, etc.)[14–17] using chemical, physical, enzymatic methods or their combination.[18,19]

Cellulose has three hydroxyl groups in its elementary structure, and the abundant hydroxyl functional groups in its macromolecules allow a wide range of functionalization via chemical reactions, leading to the development of various materials with tunable properties. Cellulose derivatives (carboxymethyl cellulose (CMC), methyl cellulose (MC), and hydroxypropyl methyl cellulose (HPMC)) are widely used for drug delivery in pharmacy, biomedicine and are considered as the first generation (nonspecific) of mucoadhesive polymers.[20] Some of them (for example, CMC) forms hydrogen bonds with mucosal membranes, and others (MC, HPMC) spread onto mucus and form the interpenetration layer with mucus gel through diffusion.[21] However, their adhesion to mucous membranes is often insufficiently strong. There are some strategies to enhance the mucoadhesive properties of conventional polymers. For example, the introduction of thiol groups into a polymer backbone allows for covalent anchoring to the mucus layer through the formation of disulfide bonds.[22] Furthermore, the acryloylate,[23] methacryloylate,[24] boronate,[25] maleimide[26,27] and aldehyde[28] groups improve mucoadhesive properties of polymers. The acryloyl group has a reactive double bond that can form a covalent linkage with the free thiol groups of cysteine residues found in mucin glycoproteins via thiol-ene click reactions occurring under physiological conditions.

A. A. Atakhanov, N. S. Ashurov, M. M. Kuzieva, B. N. Mamadiyorov, D. J. Ergashev, S. S. Rashidova
Institute of Polymer Chemistry and Physics
Uzbekistan Academy of Science
A. Kadiriy str., 7b, Tashkent 100128, Uzbekistan
E-mail: a-atakhanov@yandex.com
V. V. Khutoryanskiy
School of Pharmacy
University of Reading, Whiteknights
PO Box 224, Reading RG6 6AD, UK
E-mail: v.khutoryanskiy@reading.ac.uk

The ORCID identification number(s) for the author(s) of this article can be found under https://doi.org/10.1002/mabi.202400183

DOI: 10.1002/mabi.202400183

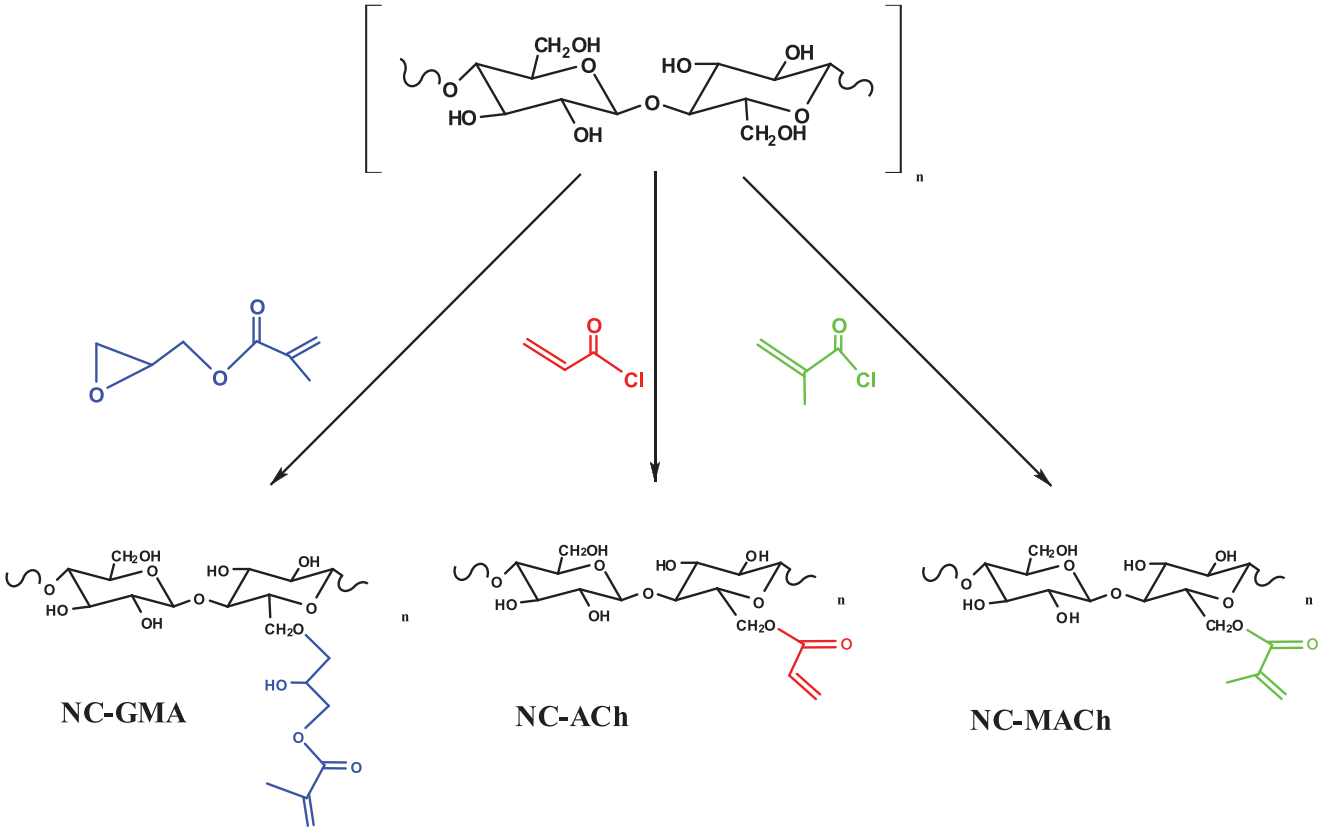

Figure 1. Reaction scheme for the synthesis of NC-GMA, NC-ACh, and NC-MACh.

NC as well as microcrystalline cellulose (MCC) can be used as an inert filler, binder, and drug delivery vehicles in pharmaceutics,[9,29] and it can be adapted for the design of mucoadhesive formulations.[30] The conjugation of the above functional groups to the NC backbone will enhance its mucoadhesive capabilities. Although the NC unit cell has three active hydroxyl groups, these hydroxyl groups play a major role in forming hydrogen bonds in the formation of fibrils, and numerous intramacromolecular hydrogen bonds limit the solubility of cellulose in many solvents. So, the majority of reactions used for the synthesis of cellulose derivatives (CMC, MC, and HPMC) usually are conducted in heterogeneous conditions.

In the present study, we synthesized acryloylated nanocellulose (NC-ACh) and methacryloylated nanocellulose (NC-MACh) derivatives and investigated their stricture and mucoadhesive properties using freshly excised sheep oral mucosa. To the best of our knowledge, this is the first study reporting the enhancement of mucoadhesive properties of NC using these strategies.

2. Results and Discussion

Three different approaches have been undertaken to introduce unsaturated groups into the structure of NC using reactions with glycidyl methacrylate, methacryloyl chloride and acryloyl chloride as shown in **Figure 1**.

For the esterification of the sterically hindered hydroxyl group electron-rich pyridines such as DMAP provide superior levels of catalytic turnover.[39,40] There are two reaction routes that explain chemical modifications of natural and synthetic polymers through the use of the GMA: transesterification and epoxide ring-opening mechanisms depending on reaction conditions.[41]

In the reactions of NC with acryloyl and methacryloyl chlorides, DMAP plays the role of a nucleophilic agent that promotes the formation of the (meta)acryloylpyridinium salt intermediate.[42] This intermediate can be attacked by hydroxyl groups of cellulose more easily, and DMAP is eliminated for the next catalytic cycle.

The H^1 NMR spectra of NC and its resulting derivatives (**Figure 2**) show the distinctive peaks typical for cellulose at δ 3.0–4.2 ppm.[43,44] With the cellulose derivatives, the new peaks at 2.25–2.75 ppm and additional peaks at 6.25 ppm are observed responsible for the protons that belong to unsaturated C=C groups of GMA, ACh, and MACh. Additionally new peak at 2.7 ppm is observed in all three derivatives due to the protons of $=CH_2$ group. Furthermore, a new peak appears in NCC-GMA conjugate at 2.3 ppm due to the protons of $C-CH_2$- group.

FT-IR spectra show characteristic absorption bands for NC (**Figure 3**) at 3400 cm^{-1}, which are related to the stretching vibrations of O–H, at 1420, 1335, 1202, 1075–1060 cm^{-1} corresponding to the bending vibrations of —CH—, $-CH_2-$, —OH, —CO, the stretching vibrations of C—O and the pyranose rings.[14] The appearance of new bands in the FTIR spectra of NC derivatives at 1721 cm^{-1} is attributed to the C=O stretching

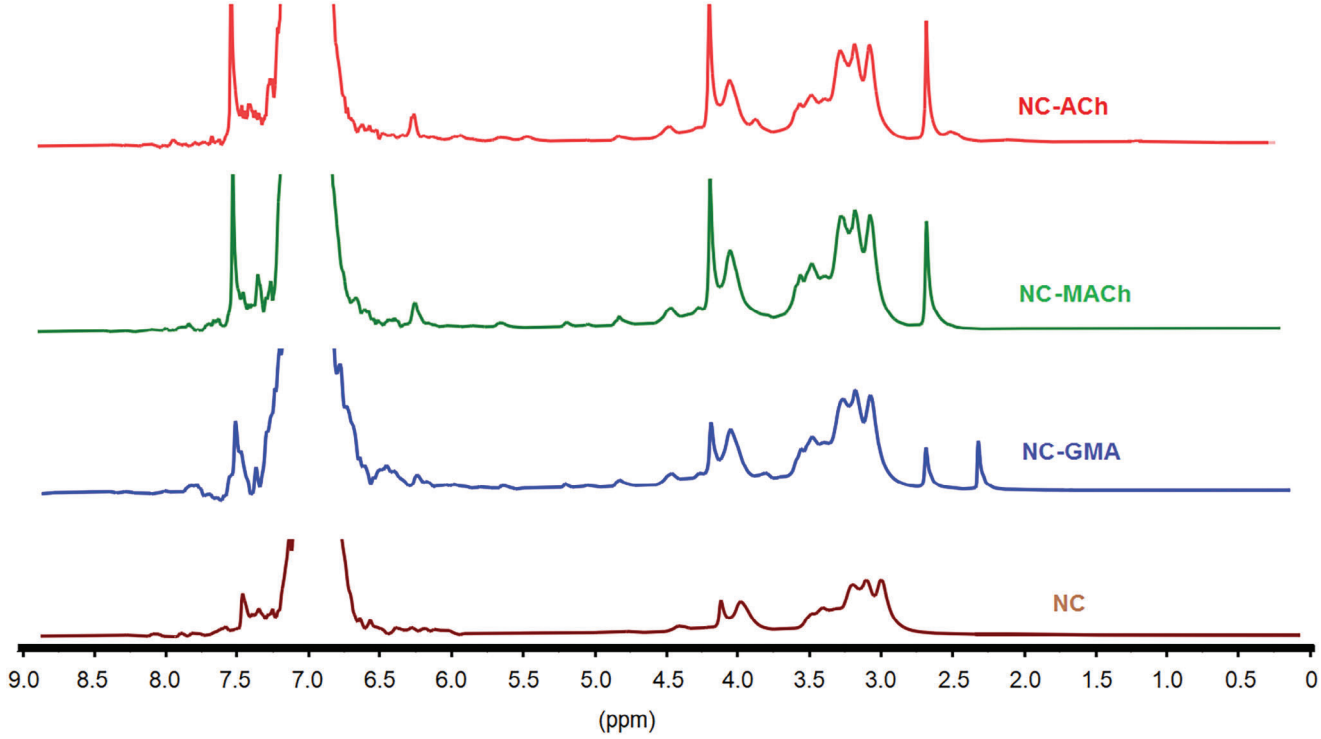

Figure 2. ^{1}H NMR spectra of NC, NC-GMA, NC-MACh and NC-ACh.

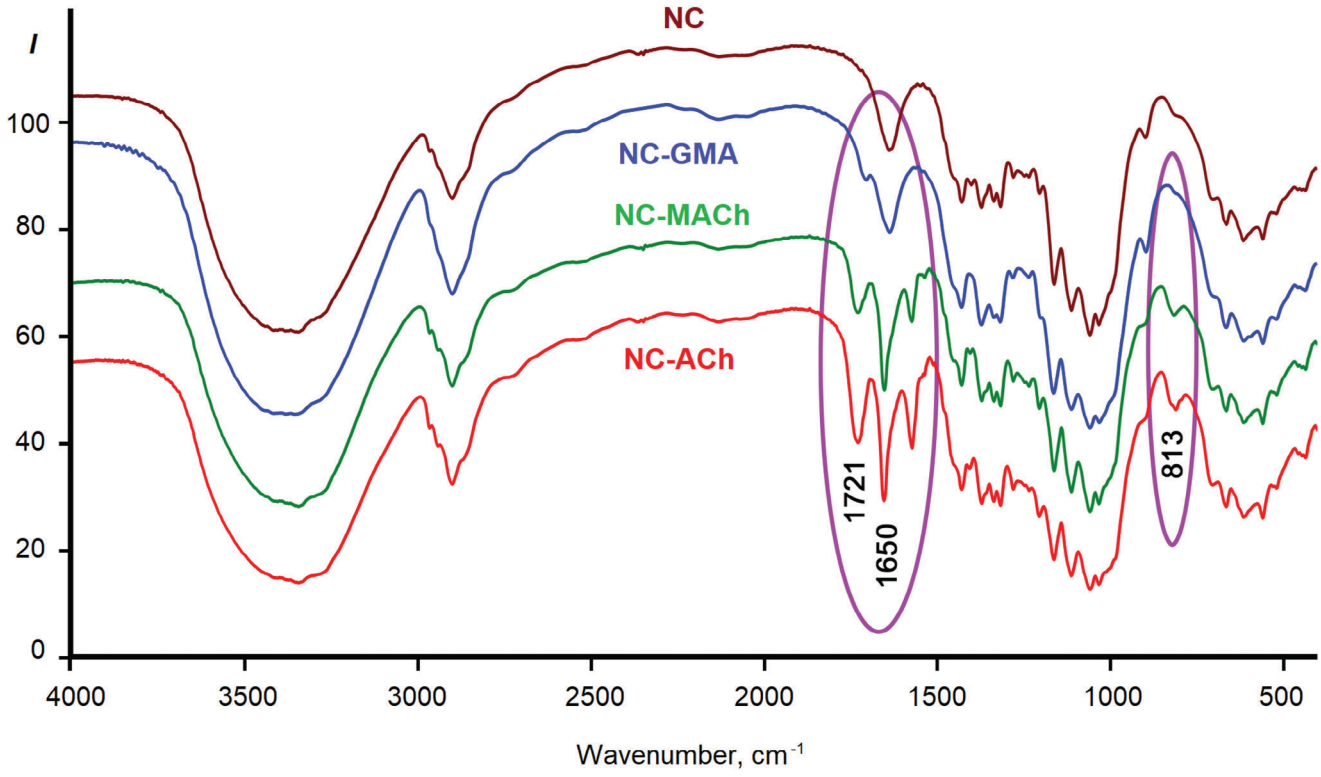

Figure 3. FTIR spectra of NC, NC-GMA, NC-ACh, and NC-MACh.

Table 1. Synthetic yield, physical properties and degrees of substitution (determined using FTIR spectroscopy) of NC derivatives.

Parameter	NC-GMA	NC-ACh	NC-MACh
Synthetic yield	51%	62%	74%
Physical appearance	white solid	white solid	white solid
Degree of substitution	11 ± 2%	25 ± 2%	17 ± 2%

frequency of conjugated ester groups,[45] and at 1650, 813 cm^{-1} indicate a double C=C bond.[33,46] The degrees of substitution were calculated using FTIR spectra by subtracting the spectra and integrating the absorption bands of the respective groups.

The physicochemical characteristics of the synthesized derivatives are presented in **Table 1**.

The results of UV spectroscopic studies show (**Figure 4**) that there are three absorbance peaks at ≈196, 226, and 290 nm associated with the C=O of the carboxyl groups (at 240, 290 nm) and the carboxyl groups (at 190–210 nm). As can be seen from the UV spectra of NC derivatives, electronic transitions π–π* and n–π* of C=O and C=C conjugated bonds are observed, which differ in intensity, in relation to the selection rules for electronic transitions. In the region of 190–230 nm, absorption bands observed are associated with π–π* transitions of electrons and a bathochromic shift towards long wavelengths occurs with an increase in the number of conjugated bonds in the chain of macromolecules. The absorption bands at 260–290 nm are associated with n-π* electronic transitions of conjugated bonds and carbonyl groups. UV spectroscopic studies have shown that there is a shift of absorption bands to the long wavelength region, which is associated with conjugated bonds. The absorption band at 350 nm is associated with n–π * electronic transitions of C=O groups, but due to the number of these groups, according to Woodward's law,[47] they are shifted to the long wavelength region.

To confirm the presence of unsaturated C=C groups qualitatively a reaction with potassium permanganate was used in aqueous suspensions of NC derivatives. Mixing these derivatives with potassium permanganate solutions results in color changes from purple to brown, which confirms the successful modification of cellulose.[34] The use of unmodified NC as a control does not result in the color changes.

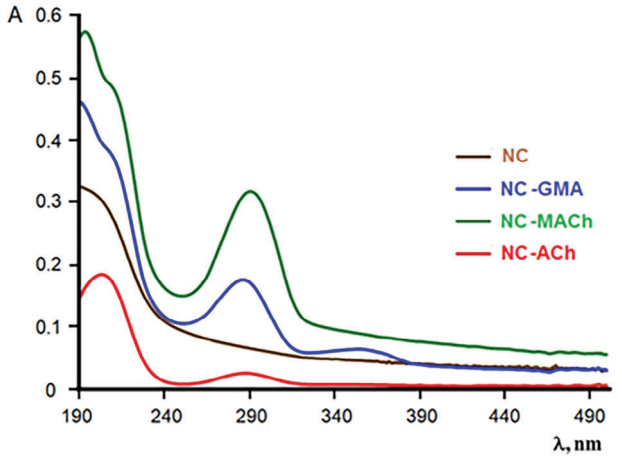

Figure 4. UV spectra of the NC, NC-GMA, NC-MACh, and NC-ACh.

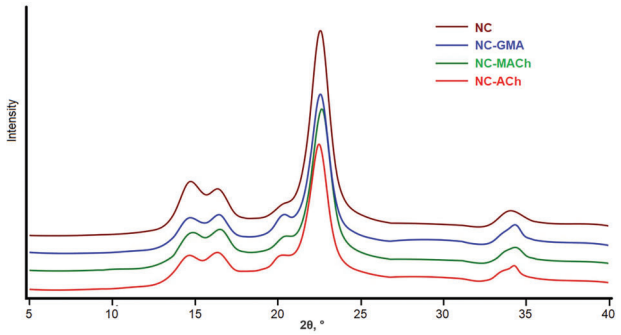

Figure 5. X-ray diffractograms of NC, NC-GMA, NC-ACh, and NC-MACh.

The X-ray diffractograms of dried NC and derivatives showed that there are four diffraction signals in the region 2θ=14°, 16°, 22° and 34°, corresponding to the planes 10, $\bar{1}$10, 200, and 004 (**Figure 5**).

The crystal index of NC derivatives was changed and they had 88% for NC, 82% for NC-GMA, 73% for NC-MACh and 63% for ACh. The modification process of NC partially disrupted the cellulose crystal structure.[48] The interplanar distances (d) of NC derivatives crystals have also increased (**Table 2**).

This also confirms the interplanar distances (d), whose values increase in the functionalized NC sample. The results of X-ray diffraction analysis show that the functionalization process affects the size of NC crystallites anisotropically, since the size of crystallites increases in one direction but does not change in another direction, which may be due to the accessibility of the surface of NC crystallites for the modifying reagent (GMA, ACh, and MACh). The chemical modification is supposed to begin at the surface of cellulose crystallites and then gradually move anisotropically into deeper layers of the crystalline structure. The use of a smaller size of the modifying reagent results in a greater degree of substitution and a lower degree of sample crystallinity.

The TGA thermograms of NC and its derivatives (**Figure 6**) showed that the weight loss for all samples proceeds in three stages. The first weight loss event upon heating to 100 °C (5–9%) is possibly related to the removal of moisture.[48,49]

The second stage is probably due to the decomposition process related to the thermal oxidation of cellulose at 200–300 °C. Although cellulose derivatives usually have a lower decomposition temperature than the parent cellulose,[33,50] in our case, NC derivatives have a higher degradation temperature than NC. It is likely due to the presence of unsaturated C=C bonds in NC derivatives. An increase in temperature leads to the polymerization of these unsaturated bonds and the formation of cross-linked structures, whose degradation temperature will be higher.[51] Samples with a higher degree of substitution of NC have greater decomposition temperatures.

The AFM study showed that NC particles have a needle-like shape with a width of 20–80 nm and a length of 180–600 nm (**Figure 7**).

The size and shape of NC particles are substantially altered following the modification, resulting in the formation of

Table 2. Structural parameters of NC and NC derivatives.

Sample	Miller indices hkl	2θ, deg.	d-spacing, Å	FWHM,°	Crystallite size τ, Å	CrI, %	Unit cell size, Å			γ, °
							a	b	c	
NC	$1\bar{1}0$	14.87	5.953	1.926	43.5	88	7.79	8.01	10.43	95.65
	110	16.51	5.362	1.995	42.1					
	012	20.44	4.341	0.901	93.0					
	102	20.74	4.298	1.546	55.3					
	200	22.77	3.901	1.279	66.2					
	023	34.22	2.618	1.927	45.2					
	004	34.61	2.589	0.630	139					
NC–GMA	$1\bar{1}0$	14.66	6.039	1.487	56.2	82	7.19	8.05	10.45	112.2
	110	16.43	5.392	1.607	52.2					
	012	20.36	4.358	1.352	62.4					
	200	22.57	3.935	1.311	64.55					
	023	30.07	2.970	3.635	23.7					
	004	34.33	2.609	1.390	62.5					
NC-ACh	$1\bar{1}0$	14.70	6.020	1.795	46.6	63	7.90	8.10	10.49	93.12
	110	16.39	5.402	1.173	72.2					
	012	19.50	4.547	12.418	6.8					
	102	20.53	4.323	1.415	60.2					
	200	22.51	3.947	1.313	64.4					
	023	33.42	2.679	0.311	282					
	004	34.21	2.619	1.328	66.4					
NC-MACh	$1\bar{1}0$	14.70	6.019	2.331	36.2	73	7.18	8.40	10.46	122.7
	110	16.53	5.359	1.125	75.4					
	012	19.07	4.650	9.349	9.0					
	102	20.85	4.256	3.408	24.8					
	200	22.66	3.921	1.281	66.0					
	004	34.16	2.622	1.560	55.6					

elongated ellipsoid particles that range in size from 200 to 350 nm. It appears that this is because the side groups of cellulose macromolecules grow in size during modification, which causes crystallites to enlarge in a direction perpendicular to the axis of macromolecules.

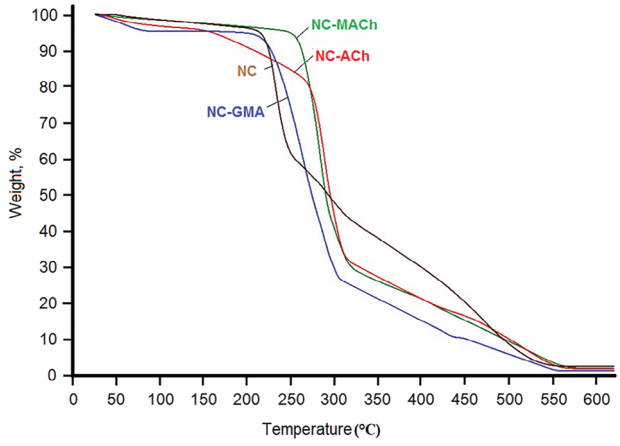

Figure 6. TGA thermograms of NC, NC-GMA, NC-Ach, and NC-MACh.

2.1. Mucoadhesion Studies

2.1.1. Retention on Sheep Oral Mucosa

The retention studies on different mucosal surfaces were described in previous publications.[26,52] In our work we carried

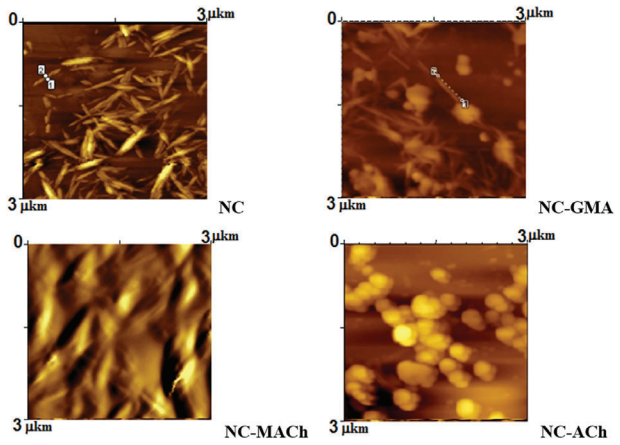

Figure 7. AFM images of NC, NC-GMA, NC-ACh, and NC-MACh.

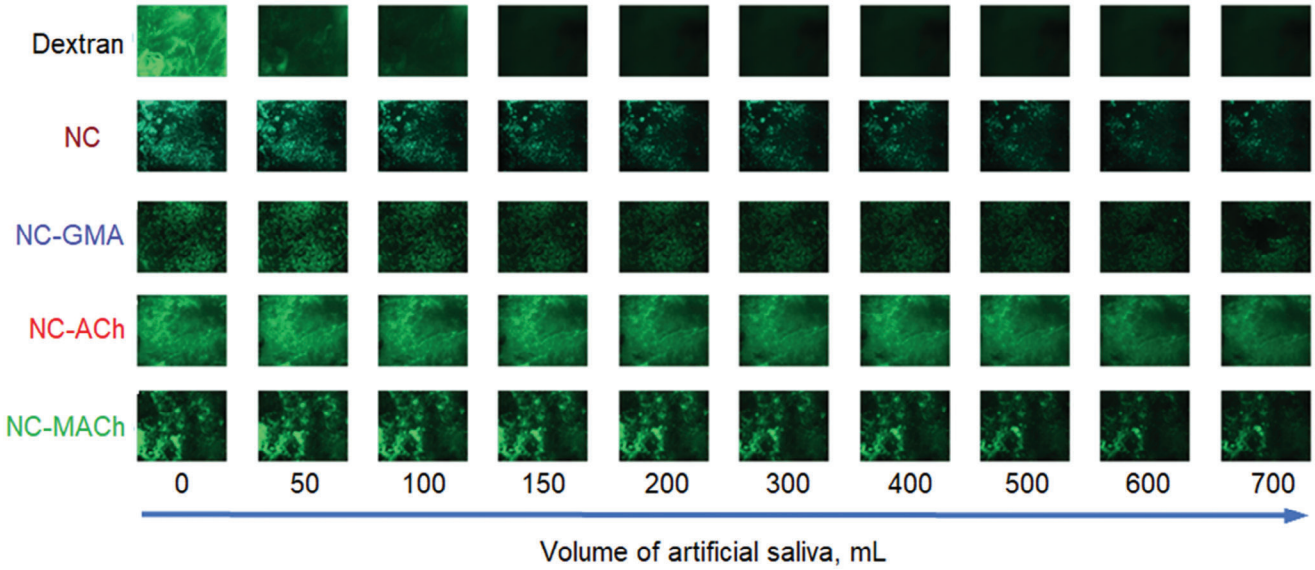

Figure 8. Exemplar microphotographs showing FITC-Dextran, NC, NC-GMA, NC-ACh, and NC-MACh washout from sheep oral tissue with artificial saliva solution. Scale bars correspond to 6 mm.

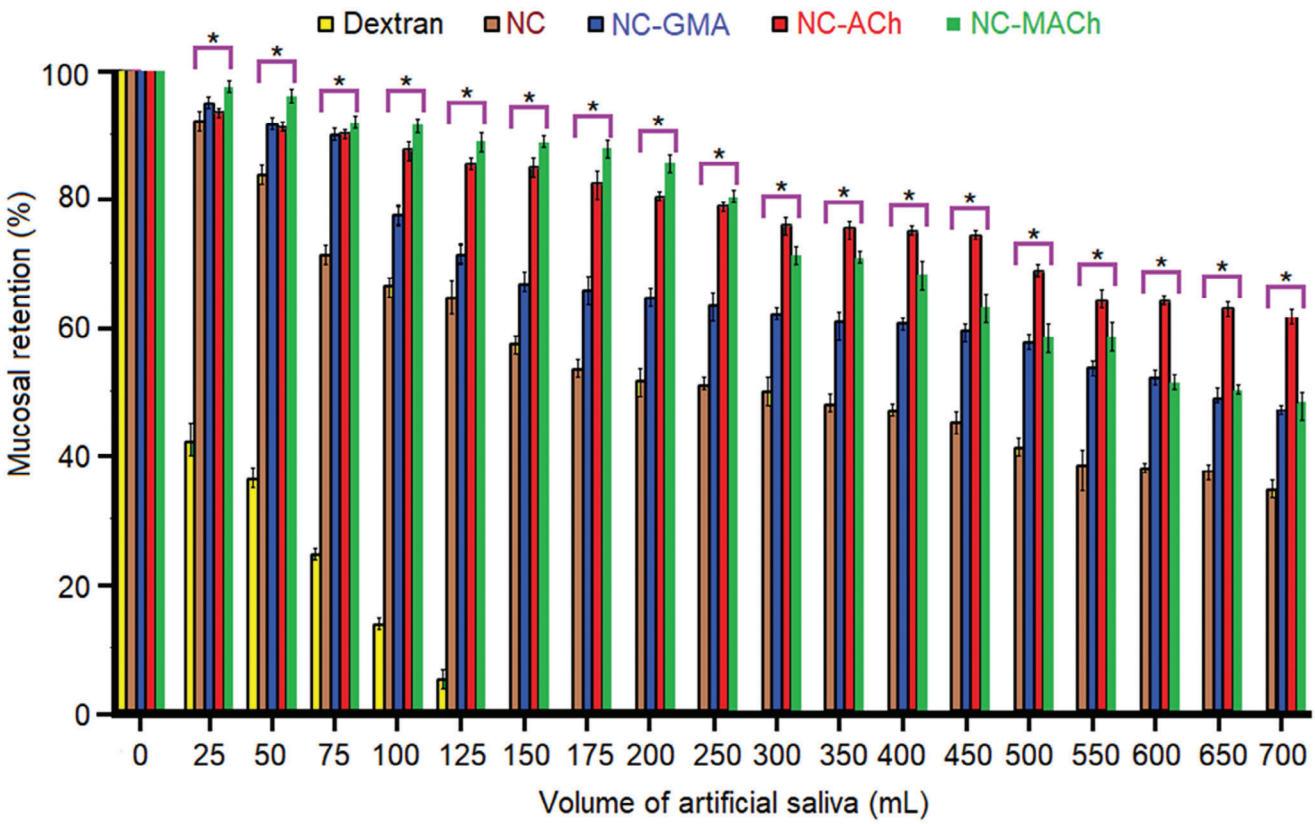

Figure 9. Mucosal retention of FITC-labeled NC-GMA, NC-MACh, and NC-Ach on sheep oral tissue; FITC-dextran served as a negative control and FITC-NC (unmodified NC) as a positive control. Result presented as mean ± standard deviation, $n = 3$, *depicts statistically significant differences between samples ($p < 0.05$).

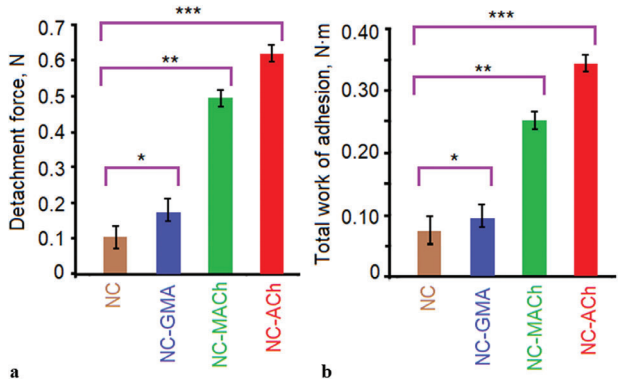

Figure 10. a) Force of detachment and b) total work of adhesion of NC, NC-GMA, NC-MACh, and NC-ACh to sheep oral mucosa measured using tensile test. Data are expressed as mean values ± standard deviations ($n = 3$). Statistically significant differences are given as: * = $p<0.05$; ** = $p<0.01$; *** = $p<0.001$.

out experiments on freshly excised sheep oral mucosa, irrigated with artificial saliva. Fluorescent images of these samples are presented in **Figure 8**.

The superior mucoadhesive behavior of all NC derivatives as shown in **Figure 9** is likely due to the presence unsaturated (meth)acrylate groups that can form covalent bonds with thiols of mucin present on the mucosal surface.[53,54]

2.1.2. Detachment from Sheep Oral Mucosa

In this method we studied the detachment of the synthesized NC derivatives from sheep oral mucosa. The force of detachment or adhesive strength is the force required to overcome the adhesive bonds between the polymer materials and mucosa, while the total work of adhesion is the area under the force–distance curves.[37]

The results showed that NC-GMA, NC-MACh, and NC-Ach were 2–6 times more mucoadhesive compared with the unmodified NC (**Figure 10**). The NC-ACh sample has the highest mucoadhesiveness that is related to its degree of substitution. Overall, the adhesive force of the polymers correlated well with their work of adhesion values as NC-MACh and NC-ACh exhibited greater force of detachment and work of adhesion relative to the neat NC.

2.1.3. Rotating Cylinder Method to Evaluate Mucoadhesive Properties

In order to evaluate the binding to the mucosa as well as the cohesiveness of the tablets, an appropriate method has been used as described by the Bernkop-Schnurch group earlier.[38] In this method the tablets were attached to the mucosal tissues secured on a rotating cylinder immersed into artificial saliva solution at 37 °C. The detachment or desintegration time of these tablets was recorded visually. The results of mucoadhesion studies performed using the rotating cylinder method are shown in **Figure 11**.

The adhesion time of the NC-ACh tablets was 9.0-fold greater, and the adhesion time of the NC-MACh tablets was 6.0-fold

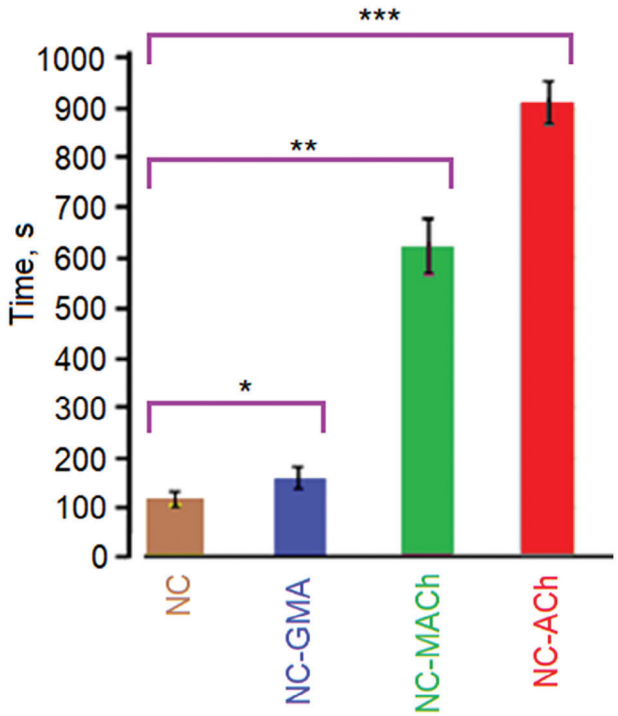

Figure 11. Comparison of the adhesion time of NC, NC-GMA, NC-MACh, and NC-ACh tablets on freshly excised sheep oral mucosa according to the rotating cylinder method in artificial saliva. Result presented as mean ± standard deviation, $n = 3$. Statistically significant differences are given as: * = $p<0.05$; ** = $p<0.01$; *** = $p<0.001$.

greater than the adhesion time of the unmodified NC. It can be explained by the formation of covalent bonds between the acryloyl groups and the thiol groups of the mucus.

All mucoadhesion studies showed that the new NC derivatives have good mucoadhesive properties and they are significantly more adhesive compared with the unmodified NC. Based on the mucoadhesiveness, all samples could be arranged in the following order: NC-ACh>NC-MACh>NC-GMA>NC. This suggests that the modified NC derivatives could be exploited further for transmucosal drug delivery due to their superior mucoadhesive features.

3. Conclusion

In this study glycidyl methacrylate, acrylate, and methacrylate groups were grafted onto NC through the heterogeneous reaction using dimethyl aminopyridine as a catalyst to synthesize novel mucoadhesive polymers.^{1}H NMR, FTIR and permanganate analysis confirmed the successful synthesis of the NC derivatives. X-ray, FTIR and TGA analysis showed that that the smaller the size of the modifying reagent, the higher the degree of substitution and the lower the degree of crystallinity. The synthesized novel NC derivatives have greater mucoadhesive properties on the sheep oral mucosa than the parent NC. New NC derivatives with enhanced mucoadhesive properties could be of interest for application in transmucosal drug delivery.

These mucoadhesive NC derivatives may be used in the future to develop formulations with various active pharmaceutical

ingredients. To the best of our knowledge, this is the first study reporting the chemical modification of NC with the aim to enhance its mucoadhesive properties.

4. Experimental Section

Materials: This study used NC (20 kDa, degree of crystallinity DC = 83%) or NC derivatives that was produced from cotton cellulose according to the protocol described previously.[31] Glycidyl methacrylate (GMA), acryloyl chloride (ACh), methacryloyl chloride (MACh), dimethyl sulfoxide (DMSO), N,N-dimethylacetamide (DMAc), hydroquinone, and potassium permanganate were purchased from Thermo Scientific (UK). 4-dimethyl-amino-pyridine (DMAP), triethyl amine (TEA) were acquired from Scientific Laboratory Supplies (UK). Fluorescein isothiocyanate (FITC)-dextran (3-5 kDa), dextran (5 kDa), dibutyltindilaurate (DBTDL), trifluoroacetic acid (TFA) were purchased from Sigma–Aldrich (UK). Disodium hydrogen phosphate, sodium chloride, potassium chloride, ammonium chloride, and calcium chloride dihydrate were all purchased from Fisher Scientific (Leicestershire, UK). All chemical reagents were used as received without further purification. Dialysis membrane with molecular weight cut off 12–14 kDa was obtained from Medicell International (London, UK). Freshly excised sheep oral tissues were received from PC Turner Abattoir (Farnborough, Hampshire, UK).

Synthesis of Nanocellulose Derivatives—Synthesis of Glycydylmethacrylated Nanocellulose (NC-GMA): NC-GMA was synthesized by reacting NC with glycydylmethacrylate using a published method with a slight modification.[32] Briefly, NC (10.0 g) was suspended in DMSO (250 mL) in a 0.5 L round-bottom flask equipped with a cover reflux condenser under a nitrogen atmosphere. The suspension was stirred during 1 h at 100 °C to activate NC. Then the temperature of the suspension was decreased to 40 °C and DMAP (0.2 g), hydroquinone (2.0 mL of 2% solution in ethanol) and GMA (0.95 mL) were added. The suspension was stirred at room temperature for 72 h, after which the reaction was terminated by adding an equimolar amount of concentrated HCl to neutralize DMAP. Then the suspension was centrifugated and the product was separated. The product was dispersed in deionized water, and purified by dialysis against 4.5 L deionized water with 6 water changes over 72 h. The final product was freeze-dried using HetoPowerDry LL3000 Freeze Dryer (Thermo Scientific, UK).

Synthesis of Acryloylated Nanocellulose (NC-ACh) and Methacryloylated Nanocellulose (NC-MACh): NC-ACh and NC-MACh were synthesized by reacting NC with acryloyl chloride and methacryloyl chloride, respectively, using a reported protocol with some modifications.[33] Briefly, NC (10.0 g) was suspended in DMAc (250 mL) and stirred at 100 °C for 1 h in 0.5 L round-bottom flask equipped with a cover reflux condenser. The slurry was then cooled to 40 °C, and DMAP (0.2 g), hydroquinone (2.0 mL of 2%-solution in ethanol) and either ACh (0.75 mL) or MACh (0.9 mL) were added. The suspension was stirred at room temperature for 72 h under a nitrogen atmosphere, after which the reaction was terminated by adding an equimolar amount of concentrated HCl to neutralize DMAP. After the suspension was centrifugated and the products were separated these were dispersed in deionized water and transferred to a dialysis tube and extensively dialyzed for 72 h against deionized water at 25 °C. The final products were lyophilized using HetoPowerDry LL3000 Freeze Dryer (Thermo Scientific, UK).

Characterization of Nanocellulose Derivatives—1H Nuclear Magnetic Resonance Spectroscopy (1H NMR): Solutions of NC derivatives (0.3% w v^{-1}) were prepared in TFA and allowed to be dissolved overnight at room temperature. The ^{1}H NMR spectra were recorded using 400 MHz Ultrashield Plus B-ACS 60 spectrometer (Bruker, UK).

Fourier Transform Infrared (FT-IR) Analysis: FT-IR spectra of dry samples were recorded with an Inventio-S IR Fourier (Bruker, Germany) using an attenuated total reflectance technique. The spectra were obtained in the range 4000–500 cm^{-1} at room temperature, with a resolution of 4 cm^{-1} and 16 scans.

X-Ray Diffractometry: The influence of the functionality of samples on the NC crystallinity was evaluated using XRD Miniflex 600 (Rigaku, Japan) with monochromatic CuKα radiation isolated by a nickel filter with a wavelength of 1.5418 Å at 40 kV and the current strength of 15 mA. Solid samples of NC, NC-GMA, NC-ACh, and NC-MACh were examined in the form of a powder, scanning from 2° to 70° with a scan step of 0.02°, generating characteristic diffractograms at the rate of 2.5 scans min^{-1}. The data processing of experimental diffraction patterns, peak deconvolution, describing the peaks used by Miller indices, peak shape, and the basis for the amorphous contribution were conducted using SmartLab Studio II software.

Atomic Force Microscopy (AFM): Morphological studies of NC and its derivatives were performed by using AFM Agilent 5500 (Agilent, USA). The silicon cantilevers with a stiffness of 9.5 N m^{-2} were used and the frequency was 262 kHz. The AFM scan area ($x - y - z$) was 3.0 – 3.0 – 1 µm.

Thermogravimetric Analysis (TGA): Thermal analysis of the dry samples was carried out with TG-DSC/DTA synchronous thermal analyzer STA PT1600 (Linseis, Germany) by heating ≈20 mg of each sample in an air atmosphere at a heating rate of 10 °C min^{-1} from 25 ° to 900 °C. The samples were loaded in aluminium pans.

UV Spectroscopy: UV spectra of NC and its derivatives were recorded with a Specord 210 UV-spectrophotometer (Analytic Jena, Germany) by using quartz cells 1 cm in diameter and 1 nm slit; the scanning range of measurement was 190–1000 nm, a scanning speed was 5 nm s^{-1}. The spectra were recorded using 1% aqueous solutions of the samples.

Permanganate Test to Qualify Unsaturated C═C groups: The quality analysis of unsaturated groups in NC derivatives was carried out using previously published method with slight modifications.[34] Briefly, 0.1 g NC derivative was suspended in 20 mL deionized water and left stirring for 2 h. To this suspension 3 mL of 0.1 N potassium permanganate was added, followed with the addition of 4 mL of 0.1 N oxalic acid from a microburette and the suspension was stirred for 15 min. This resulted in a change of solution color from purple to brown, which was used as a titration endpoint. The presence of small quantities of unsaturated bonds in the NC derivatives resulted in reduction of some MnO_4^- ions to Mn^{2+}, which act as a catalyst and speed up the reaction of permanganate ions with oxalic acid added subsequently.

Ex Vivo Sheep Mucoadhesion Studies—Preparation of Artificial Saliva Fluid: Artificial saliva fluid used to wash a mucosal surface was prepared as reported previously.[35] It was composed of NaCl (0.43 g), $CaCl_2$ (0.22 g), KCl (0.75 g), $NaHCO_3$ (0.20 g) and KH_2PO_4 (0.9 g) dissolved in 1 L of deionized water, pH 6.75 and the solution was kept at 37 °C throughout the experiments.

Fluorescent Labelling of Nanocellulose Derivatives: NC and its derivatives were labelled with fluorescein isothiocyanate (FITC) using a slightly modified reported procedure.[36] Briefly, 1 g of NC derivative (NC-GMA, NC-ACh, NC-MACh) was suspended in 100 mL DMSO and the mixture was stirred for 30 min at 90 °C under nitrogen atmosphere until it was homogeneously mixed. 0.01 g of fluorescein isothiocyanate was added and stirred for 10 min and 0.3% of dibutyltin dilaurate was added subsequently. The mixture was further stirred for 4 h at 90 °C. The product was washed with acetone 3 times and the precipitate was dialyzed in deionized water for 3 days. The dialyzed product was centrifuged and separated from liquid. The product was then freeze-dried.

Retention on Sheep Oral Mucosa: Fluorescence microscopy (MZ10F microscope; Leica Microsystems, Milton Keynes, UK), coupled to an "ET GFP" filter camera (Zeiss Imager A1/AxioCamMRm camera, 1296 × 966 pixels, 0.8 × magnification) was used to investigate the mucosal retention of fluorescein sodium in the presence of the polymeric carriers based on a slightly modified protocol reported by Kolawole et al.[37] Freshly excised sheep oral tissue stored on ice was used in this study within 24 h of procurement. The mucosal side of the oral tissue was preserved during excision of the required section (≈1.5 × 2.5 cm) and rinsed with artificial saliva solution (~3 mL) prior to blank tissue imaging. The mucosal tissue was placed on a 75 mm × 25 mm glass slide and maintained in an incubator at 37 °C during saliva wash-out. Initially, fluorescence images of mucosal tissues were recorded for each sample as

a background fluorescence intensity. Microscopic images were recorded for each tissue section before and after applying 100 µL of the polymer sample as well as after each of the five washing cycles with 10 mL artificial saliva/cycle at 2 mL mi(1n. The studies were carried out in triplicates. Image J software (National Institute of Health, USA) was used to analyze the microscopic images, generating average fluorescence values as a function of saliva volume used for the wash-out. To normalize the mean fluorescence values, fluorescence values obtained based on blank tissues were deducted from fluorescence values obtained after each wash out cycle while the value "1" was used to depict the fluorescence intensity from the tissue prior to wash. Suspension of the unmodified NC in deionized water (0.01 mg mL^{-1}) was used as the positive control, while dextran with poor mucoadhesive properties served as the negative control.

Tablet Preparation: The NC and its derivatives powders were compressed into tablets using a Riva Minipress (Hampshire, UK), single punch tablet press (Riva, Hampshire, UK) filled manually and press settings selected to preserve similar tablet strength between batches using a force of 8000 N. An average weight of the tablets was 50±1 mg with an average thickness of 1.00±0.01 mm and the average diameter of 10.0±0.3 mm. The average hardness of the tablets was 197±5 N.

Tensile Method: The TA-XT Plus Texture Analyser (Stable Micro Systems Ltd., Godalming, UK) coupled to a 5 kg load cell was used to study the mucoadhesive properties of the polymer samples using a slightly modified procedure reported in Ref. [37] The adhesion force that occurred between the mucoadhesive tablets and the mucous membrane was examined by measuring the force used to detach the polymer tablets from the tissue. NC tablet served as the positive control. The tablets were attached to the probe with an adhesive tape, while the sliced sheep oral tissue was secured at the base of a cylindrical container and wetted with artificial saliva fluid. The test conditions included the following: pre-speed test 1.0 mm s^{-1}; test speed 0.1 mm s^{-1}; post-test speed 0.1 mm s^{-1}; applied force 0.05 N; contact time 10.0 s; trigger type auto; trigger force 0.1 N; and return distance of 10.0 mm. Sheep mucosal tissues were maintained in an incubator at 37 °C for 10 min prior to the study.

T.A. Exponent software was used to record the area under the force versus distance curves (total work of adhesion) as well as the force of adhesion/adhesive strength which is the maximum force needed to detach the tablets from the tissue.

Rotating Cylinder Method: The rotating cylinder method was used as an additional technique to study the mucoadhesive properties of the polymer samples using the slightly modified reported protocol.[38] The tablets were attached to freshly excised sheep oral mucosa, which has been secured on a stainless-steel cylinder (diameter: 2.4 cm; height: 3.8 cm). Thereafter, the cylinder was placed in the Varian 705DS dissolution apparatus (Varian, UK) containing 500 mL artificial saliva solution at 37±1 °C. The fully immersed cylinder was rotated at 60 rpm. The detachment time of tablets was evaluated visually. Each polymer sample was evaluated in triplicates.

Statistical Analysis: All experimental data were collected in triplicates and data were expressed as the mean ± standard deviation. Data were compared using a one-way ANOVA with a post-Bonferroni test using GraphPad Prism 5.04 (GraphPad Software Inc., San Diego, California), with $p<0.05$ depicting significant differences between data sets.

Acknowledgements

The authors acknowledge the Ministry of Higher Education, Science and Innovation of the Republic of Uzbekistan for supporting A.A.A.'s visit to the University of Reading. The authors are grateful to researchers of the Institute of Polymer Chemistry and Physics (Laboratory of Physics and Physico-Chemical Methods of Investigation) for their technical help with the structural analysis of samples. Chemical Analysis Facility (University of Reading) is also acknowledged for providing access to ^{1}H NMR spectroscopy. V.V.K. acknowledges the Royal Society for his industry fellowship (IF\R2\222031).

Conflict of Interest

The authors declare no conflict of interest.

Data Availability Statement

The data that support the findings of this study are available from the corresponding authors upon reasonable request.

Keywords

acryloylation, drug delivery, methacryloylation, mucoadhesion, nanocellulose, nanoparticles

Received: April 16, 2024
Revised: July 24, 2024
Published online:

[1] N. Hoenich, *BioResource* **2006**, *1*, 270.
[2] T. Aziz, A. Farid, F. Haq, M. Kiran, A. Ullah, K. Zhang, C. Li, S. Ghazanfar, H. Sun, R. Ullah, A. Ali, M. Muzammal, M. Shah, N. Akhtar, S. Selim, N. Hagagy, M. Samy, S. K. Al Jaouni, *Polymers* **2022**, *14*, 3206.
[3] S. Kalia, A. Dufresne, B. Mathew Cherian, B. S. Kaith, L. Averous, J. Njuguna, E. Nassiopoulos, *Int J Polym Sci* **2011**, *1*, 837875.
[4] O. A. Titton Dias, S. Konar, A. L. Leão, W. Yang, J. Tjong, M. Sain, *Front Chem* **2020**, *8*, 420.
[5] V. Edwards, N. Prevost, A. French, M. Concha, A. De Lucca, Q. Wu, *Engineering* **2013**, *5*, 20.
[6] N. M. F. Hakimi, S. H. Lee, W. C. Lum, S. F. Mohamad, S. O. Al Edrus, B. D. Park, A. Azmi, *Polymers* **2021**, *13*, 3241.
[7] M. I. Voronova, O. V. Surov, M. K. Kuziyeva, A. A. Atakhanov, *Chem.Chem.Tech* **2022**, *65*,95.
[8] K. Y. Lee, Y. Aitomki, L. A. Berglund, K. Oksman, A. Bismarck, *Compos. Sci. Technol.* **2014**, *105*, 15.
[9] M. Q. Saidmuhamedova, I. H. Turdiqulov, A. A. Atakhanov, N. Sh. Ashurov, M. Abdurazakov, S. Sh. Rashidova, O. V. Surov, *Eurasian J. Chem.* **2023**, *110*, 94.
[10] M. E. Putri, A. Y. Chaerunisaa, M. Abdassah, *Indones. J. Pharm.* **2020**, *2*, 43.
[11] M. Jorfi, E. J. Foster, *J. Appl. Polym. Sci.* **2015**, *132*, 41719.
[12] N. Lin, A. Dufresne, *Eur. Polym. J.* **2014**, *59*, 302.
[13] Y. Lu, H. L. Tekinalp, C. C. Eberle, W. Peter, A. K. Naskar, S. Ozcan, *Tapi J* **2014**, *13*, 47.
[14] D. Trache, M. H. Hussin, M. M. Haafiz, V. K. Thakur, *Nanoscale* **2017**, *9*, 1763.
[15] A. A. Atakhanov, B. Mamadiyorov, M. Kuzieva, S. M. Yugay, S. Shahobutdinov, N. Sh. Ashurov, M. Abdurazzakov, *J. Khimiya Rastitel'nogo Syr'ya.* **2019**, *3*, 5.
[16] L. H. Zaini, M. Jonoobi, P. Tahir, S. Karimi, *J Biomater Nanobiotechnol* **2013**, *4*, 37.
[17] J. I. Moran, V. A. Alvarez, V. P. Cyras, A. Vazquez, *Cellulose* **2008**, *15*, 149.
[18] Y. Wang, X. Wei, J. Li, F. Wang, Q. Wang, L. Kong, *J. Mater. Sci. Chem. Eng.* **2013**, *1*, 49.
[19] X. Tong, W. Shen, X. Chen, M. Jia, J. C. Roux, *J. Appl. Polym. Sci.* **2020**, *137*, 48407.
[20] R. P. Brannigan, V. V. Khutoryanskiy, *Macromol. Biosci.* **2019**, *19*, 1900194.
[21] V. V. Khutoryanskiy, *Macromol. Biosci.* **2011**, *11*, 748.
[22] A. Bernkop-Schnürch, *Adv. Drug Delivery Rev.* **2005**, *57*, 1569.

[23] M. Davidovich-Pinhas, H. Bianco-Peled, *J Mater Sci Mater Med* **2010**, *21*, 2027.
[24] O. M. Kolawole, W. M. Lau, V. V. Khutoryanskiy, *Int J Pharm* **2018**, *550*, 123.
[25] A. E. Ivanov, *Mucoadhesive Materials and Drug Delivery Systems*, (Ed: V. V. Khutoryanskiy), John Wiley & Sons Ltd., Chichester, UK **2014**, p. 279.
[26] D. B. Kaldybekov, P. Tonglairoum, P. Opanasopit, V. V. Khutoryanskiy, *Eur. J. Pharm. Sci.* **2018**, *111*, 83.
[27] C. Pornpitchanarong, T. Rojanarata, P. Opanasopit, T. Ngawhirunpat, M. Bradley, P. Patrojanasophon, *Carbohydr. Polym.* **2022**, *288*, 119368.
[28] E. E. Brotherton, T. J. Neal, D. B. Kaldybekov, M. J. Smallridge, V. V. Khutoryanskiy, S. Armes, *Chem. Sci.* **2022**, *13*, 6888.
[29] D. V. Plackett, K. Letchford, J. K. Jackson, H. M. Burt, *Nord. Pulp Pap. Res. J.* **2014**, *29*, 105.
[30] A. Moraru, F. Oancea, *Sci. Bullet. Series F. Biotechnol.* **2022**, *16*, 137.
[31] A. A. Atakhanov, A. A. Kholmuminov, B. N. Mamadierov, I. Kh. Turdikulov, N. Sh. Ashurov, *Polym. Sci. Series A.* **2020**, *62*, 213.
[32] W. N. E. Dijk-Wolthuis, O. Franssen, H. Talsma, M. J. Steenbergen, J. J. K. Bosch, W. E. Hennink, *Macromolecules* **1995**, *28*, 6317.
[33] Y. Qian, N. Han, Y. Bo, L. Tan, L. Zhang, X. Zhang, *Carbohydr. Polym.* **2018**, *193*, 129.
[34] N. N. Porfiryeva, S. F. Nasibullin, S. G. Abdullina, I. K. Tukhbatullina, R. I. Moustafine, V. V. Khutoryanskiy, *Int. J. Pharm.* **2019**, *562*, 241.
[35] K. D. Madsen, C. Sander, S. Baldursdottir, A. M. L. Pedersen, J. Jacobsen, *Int. J. Pharm.* **2013**, *448*, 373.
[36] H. H. Cho, J. H. Choi, S. Y. Been, N. Kim, J. M. Choi, W. Kim, D. Kim, J. J. Jung, J. E. Song, G. Khang, *Int. J. Biolog. Macromol.* **2020**, *164*, 2804.
[37] O. M. Kolawole, W. M. Lau, V. V. Khutoryanskiy, *J. Pharm. Sci.* **2019**, *108*, 3046.
[38] J. Hombach, T. F. Palmberger, A. Bernkop-Schnurch, *J. Pharm. Sci.* **2009**, *98*, 555.
[39] A. V. Reis, *Int. J. Pharm.* **2003**, *267*, 13.
[40] L. Ferreira, *Carbohydr. Polym.* **2000**, *41*, 15.
[41] A. V. Reis, *J. Org. Chem.* **2009**, *74*, 3750.
[42] L. Vervoort, G. V. Mooter, P. Augustijns, R. Busson, S. Toppet, R. Kinget, *Pharm. Res.* **1997**, *14*, 1730.
[43] A. Isogai, *Cellulose* **1997**, *4*, 99.
[44] F. Jiang, J. L. Dallas, B. Kollbe Ahn, Y. L. Hsieh, *Carbohydr. Polym.* **2014**, *110*, 360.
[45] M. R. Guilherme, A. V. Reis, S. H. Takahashi, A. F. Rubira, J. P. A. Feitosa, E. C. Muniz, *Carbohydr. Polym.* **2005**, *61*, 464.
[46] X. Peng, J. Ren, L. Zhong, R. Sun, W. Shi, B. Hu, *Cellulose* **2012**, *19*, 1361.
[47] D. J. Ager, M. B. East, *Asymmetric Synthetic Methodology* (Eds: D.J. Ager), CRC Press, Boca Raton, FL, USA **1996**.
[48] M. Kuziyeva, A. Atakhanov, S. Shakhobutdinov, N. Ashurov, K. Yunusov, J. Guohua, *Cellulose* **2023**, *30*, 5657.
[49] H. Kargarzadeh, I. Ahmad, I. Abdullah, *Cellulose* **2012**, *19*, 855.
[50] M. Sakhawy, H.-A. S. Tohamy, A. S. Salama, S. Kamel, *Cellulose Chem. Technol.* **2019**, *53*, 667.
[51] M. Lin, A. Chen, *Polymer* **1993**, *34*, 389.
[52] T. M. Ways, W. M. Lau, V. V. Khutoryanskiy, *Polymers.* **2018**, *10*, 267.
[53] Y. Shitrit, H. Bianco-Peled, *Int. J. Pharm.* **2017**, *517*, 247.
[54] A. Bernkop-Schnurch, S. Steininger, *Int. J. Pharm.* **2000**, *194*, 239.